Proceedings of the 28th IEEE
EMBS Annual International Conference
New York City, USA, Aug 30-Sept 3, 2006

Distinguishing Lesions from Posterior Acoustic Shadowing in Breast Ultrasound via Non-Linear Dimensionality Reduction

Anant Madabhushi
Dept. of Biomedical Engineering,
Rutgers University
Piscataway, NJ 08854, USA
anantm@rci.rutgers.edu

Peng Yang
Dept. of Computer Science,
Rutgers University
Piscataway, NJ 08854, USA
pengyang@eden.rutgers.edu

Mark Rosen, Susan Weinstein
Dept. of Radiology
University of Pennsylvania
Philadelphia, PA 19104, USA
Mark.Rosen@uphs.upenn.edu

***Abstract*— Breast ultrasound (US) in conjunction with digital mammography has come to be regarded as the gold standard for breast cancer diagnosis. While breast US has certain advantages over digital mammography, it suffers from image artifacts such as posterior acoustic shadowing (PAS), presence of which often obfuscates lesion margins. Since classification of lesions as either malignant or benign is largely dictated by lesion's shape and margin characteristics, it is important to distinguish lesion area from PAS. This paper represents the first attempt to extract and identify those image features that can help distinguish between lesion and PAS. Our methodology comprises of extracting over 100 statistical, gradient, and Gabor features at multiple scales and orientations at every pixel in the breast US image. Adaboost, a powerful feature ensemble technique is used to discriminate between lesions and PAS by combining the different image features. A non-linear dimensionality reduction method called *Graph Embedding* is then used to visualize separation and inter-class dependencies between lesions and PAS in a lower dimensional space. Results of quantitative evaluation on a database of 45 breast US images indicate that our methodology allows for greater discriminability between the lesion and PAS classes compared to that achievable by any individual image texture or intensity feature.**

***Index Terms*— Breast, ultrasound, posterior acoustic shadowing, AdaBoost, non-linear dimensionality reduction, lesion.**

I. Introduction

Breast ultrasound (US) is used for screening women with dense breasts since this is difficult to do using routine mammography [2], [3]. Breast US can also diagnose cysts with an accuracy approaching 100% [1]. It has been shown that the shape and margin characteristics of the lesion are the most important factors in discriminating between benign and malignant lesions [1]. Several researchers have proposed computer-aided diagnosis (CAD) algorithms for detecting lesions as well as distinguishing between benign and malignant lesions [2], [3], [5] on breast US and digital mammography. One of the major issues for CAD on breast US has been the presence of acoustic artifacts such as speckle and posterior acoustic shadowing (PAS). PAS typically appears as a dark vertical patch immediately posterior to the lesion (Figure 1(a)). Owing to the similarity in intensity characteristics between most hyper-echoic lesions and PAS, lesion margins often get obfuscated making it difficult to accurately determine lesion shape and hence classify the lesion as benign or cancerous. Precisely such a scenario is displayed in Figure 1(a), where the lower boundary of a lesion is indistinguishable from PAS. Figures 1(b) and (c) show the corresponding expert (radiologist) segmentations for the lesion and PAS. Figure 1(d) which shows the overlap between the expert segmentations of the lesion and PAS in Figures 1(b), (c) reveals the problem difficulty, even for an expert radiologist.

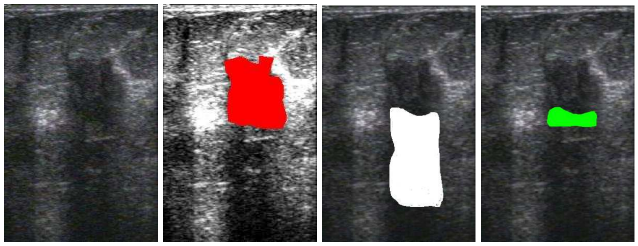

(a) (b) (c) (d)

Fig. 1. (a) Original breast US image with PAS obfuscating lower lesion margin. Expert segmentations of (b) lesion and (c) PAS in (a). (d) Overlap of lesion and PAS segmentations in (b), (c) reveals the difficulty of the problem.

Most CAD work in breast US has sidestepped the issue of PAS [3]. Drukker *et al.* [5] attempted to analyze PAS in breast US by investigating the skewness values within manually defined regions of interest. No explicit attempt, however, was made to identify intensity or textural differences between lesion area and PAS. The motivation behind this paper is to identify those image attributes that can help (a) improve discriminability between lesions and PAS, and (b) to visualize the dependencies between pixels belonging to the lesion and PAS classes in a lower dimensional space. Our methodology involves extracting over 100 statistical, steerable, and gradient texture features at multiple scales and orientations at every image pixel. Bayes Theorem [6] is used to assign a vector of likelihoods to each image pixel of belonging to the lesion or PAS class based on the extracted image features. Adaboost [7], a powerful feature ensemble method is used to selectively combine the most discriminating textural and intensity features. A non-linear dimensionality reduction technique called *Graph Embedding* [4] is then used to visualize the differences between lesion and PAS classes in a lower dimensional space. The ability to discriminate between the lesion and PAS classes

has significant clinical implications in that it could help improve the diagnostic ability of an expert radiologist or an automated CAD technique.

The organization of the rest of this paper is as follows. In Section II we describe the details of our methodology. In Section III we present our results (qualitative and quantitative) and our concluding remarks are presented in Section IV.

II. Methodology

A. System Overview

Following data acquisition and manual segmentation of lesion and PAS areas on breast US, over a 100 texture features are extracted from within the manually segmented regions. Probability density functions (pdfs) for each of the extracted features are then generated in the Training module. Each image pixel is then assigned a conditional likelihood of belonging to the lesion or PAS class using Bayes Theorem [6] and the extracted attributes. The conditional likelihoods for each texture feature are then combined to produce a joint likelihood in the Feature Combination module. Graph embedding is then performed to visualize dependencies between lesion and PAS classes in the lower dimensional space. The flowchart in Figure 2 shows the different components comprising the system.

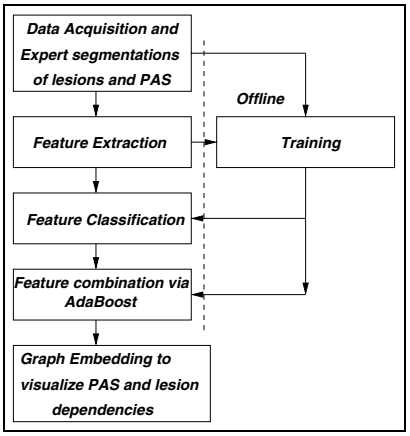

Fig. 2. Flowchart showing individual modules and system flow.

B. Feature Extraction

We represent a breast US image by a pair $\mathcal{C} = (C, g)$, where C is a 2-dimensional array of pixels and g is the image intensity function. The application of K different texture operators ϕ_γ, for $1 \leq \gamma \leq K$, on $\mathcal{C}$ results in K corresponding feature scenes $F_\gamma = (C, f_\gamma)$. Hence each pixel $c \in C$ is described by a K dimensional feature vector $\Phi(c) = \{f_1(c), f_2(c), ..., f_K(c)\}$. A total of 114 texture features at multiple scales and orientations were extracted from each of 45 breast US images in our database. The features included (1) 12 first order statistical features (mean, median, average, and standard deviation of image intensity at 3 different scales), (2) 13 second order statistical Haralick features, (3) 80 Gabor features at 10 different scales and 8 different orientations, and (4) 9 gradient features including the Sobel and Kirsh features. Figures 3(b)-(f) shows some representative feature scenes for the breast US image shown in Figure 3(a).

C. Training

Two expert radiologists at the Hospital at the University of Pennsylvania manually segmented areas corresponding to lesions and PAS on 45 B-mode breast US images. These 45 images comprised both malignant and benign lesions. Ten training images were used to generate probability distribution functions (pdf's) $p(c, f_\gamma | \omega_L)$, for $1 \leq \gamma \leq K$, for each of the extracted features ϕ_γ for the lesion class ω_L.

D. Feature classification

From Bayes rule [6], the posterior conditional probability $P(\omega_L | c, f)$ that a pixel $c \in C$ belongs to the lesion class ω_L given the associated feature $f(c)$ is given as

$$P(\omega_L | c, f) = \frac{P(\omega_L) p(c, f | \omega_L)}{\sum_{j \in \{L,S\}} P(\omega_j) p(c, f | \omega_j)}, \qquad (1)$$

where $p(c, f | \omega_j)$ is *a-priori* conditional density associated with feature f for ω_L and the PAS class (ω_S). $P(\omega_L)$, $P(\omega_S)$ are the prior probabilities of observing objects (pixels) belonging to ω_L and ω_S. Hence each pixel $c \in C$ is associated with a *likelihood vector* $\Pi^L = [P(\omega_L | c, f_\gamma) \mid \gamma \in \{1,2,..,K\}]$ containing the posterior conditional probabilities that c belongs to the lesion class ω_L.

E. Feature Combination

Adaptive Boosting (AdaBoost) proposed by Freund and Schapire [7] is a feature ensemble method in which sequential classifiers are generated for a certain number of trials (T) and at each iteration (t) the weights of the training dataset are changed based on the base classifiers ($P(\omega_L | c, f_t)$) that were previously selected. The final Boosted classifier for class ω_L at each pixel $c \in C$ is obtained as a weighted (α_t) combination of the base classifiers, $\mathcal{P}^L(c) = \sum_{t=1}^{T} \alpha_t P(\omega_L | c, f_t)$. Hence for $c \in C$, $\mathcal{P}^L(c)$ represents the combined likelihood that c belongs to lesion class ω_L.

F. Graph Embedding to Visualize Class Separability

The aim of Graph embedding is to find a placement vector $X(c)$ for each pixel $c \in C$ such that the distance between c and the lesion class ω_L that it belongs to are monotonically related to the combined posterior probability $\mathcal{P}^L(c)$ in a low-dimensional space [4]. If two pixels c, d both belong to class ω_L, then $[X(c) - X(d)]^2$ should be small. To compute the optimal embedding, we first define a confusion matrix W to represent the similarity between any two objects $c, d \in C$ in a high dimensional feature space.

$$W(c, d) = e^{-\|\mathcal{P}^L(c) - \mathcal{P}^L(d)\| \in R^{|C| \times |C|}} \qquad (2)$$

Computing the embedding is identical to optimization of the following function

$$E_{w_L}(X) = 2\zeta \frac{X^T (D - W) X}{X^T D X}, \qquad (3)$$

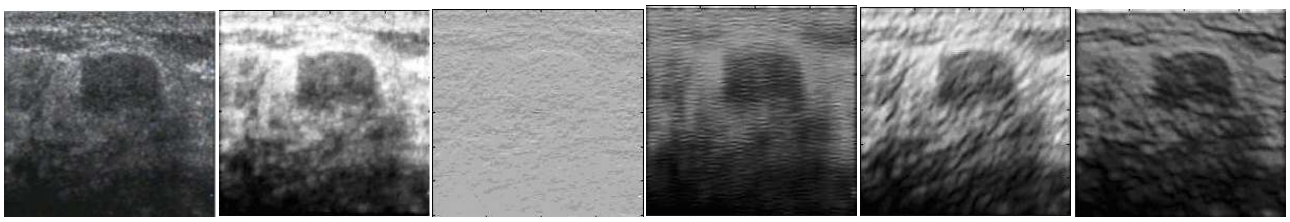

(a) (b) (c) (d) (e) (f)

Fig. 3. (a) Original breast US image and corresponding feature scenes for (b) median intensity, (c) directional gradient, (d) entropy, and (e), (f) Gabor feature scenes at 2 different scales and orientations.

where $D(c,d) \in R^{|C|\times|C|}$ is a diagonal matrix with $D(c,d) = \sum_{c,d} W(c,d)$, $\zeta = |C| - 1$ and $|C|$ represents the cardinality of set C. The global energy minimum of this function is achieved by the eigenvector corresponding to the second smallest eigenvalue of,

$$(D - W)X = \zeta DX. \tag{4}$$

For pixel $c \in C$, the embedding $X(c)$ has the coordinates of c in the embedding space and given as,

$$X(c) = [e_\kappa(c)|\kappa \in \{1, 2, .., A\}], \tag{5}$$

where $e_\kappa(c)$ are the first A eigen values associated with c in the embedding space. Note that graph embedding differs from other dimensionality reduction methods such as PCA in that object adjacency's in the high dimensional space are preserved in the low dimensional embedding space.

III. Results

We present below both qualitative and quantitative results of our experiments on a database of 45 breast US images for which manually segmented masks of lesion and PAS were available. Of these images, 10 were used for training while 35 images were used for evaluation. Since pdf's for ω_L were generated by determining feature values at every pixel, 10 training images were found to be sufficient to capture the range of feature variations for ω_L and ω_S. Quantitative evaluation was done to (1) compare discrimination accuracy between lesion and PAS obtained by AdaBoost versus that obtained by using the individual texture features, and (2) to visualize lesion and PAS separability in the low dimensional embedding space.

A. Discriminability between lesion and PAS

Receiver Operating Characteristic (ROC) curves were used to compare lesion classification accuracy by using the Boosted classifier versus using the individual base features (weak classifiers). In Figure 4 are shown the average ROC curves for the AdaBoost classifier (green circles) and the 114 individual base classifiers (solid blue lines) obtained for 35 test images. As can be discerned by the area under the ROC curves, the Boosted classifier produces significantly higher discrimination accuracy between lesion and shadowing compared to any of the base classifiers. In fact Figure 4 suggests that the performance of the individual classifiers in distinguishing the 2 classes is at best random (ROC curves lie on the diagonal 45^o line) and explains why radiologists using a single base classifier (image intensity) have a difficult time distinguishing the two classes.

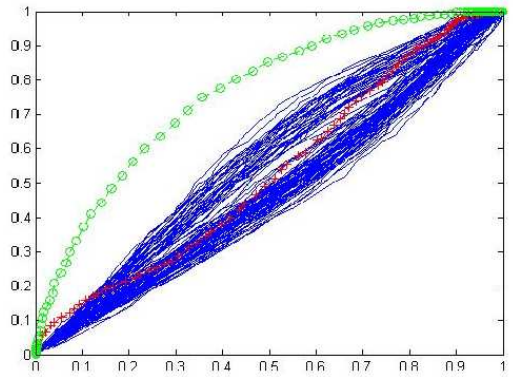

Fig. 4. ROC curves comparing accuracy of AdaBoost (green circles) and individual classifi ers (blue lines) in detecting lesions. The larger area under the ROC curve for the AdaBoost classifi er clearly suggests the improved discriminability between the two classes compared to the base classifi ers.

B. Visualizing Class Separability in Embedding Space

Figures 5(a), (e), and (i) shows three different breast US images, along with the corresponding lesion (red) and shadowing masks (white) segmented by 2 trained radiologists (Figures 5 (b), (f), and (j)). In order to visualize discriminability of the Boosted classifier in the embedding space we plotted (Figures 5(c), (g), (k)) the principal eigen values (e_2 versus e_3) for different pixels $c \in C$ corresponding to classes ω_L (red circles) and ω_S (black dots) for the 3 breast US images in Figures 5 (a), (e), and (i). The embedding plots for all 3 images show a clear separation between the lesion and PAS classes (The ellipses in Figures 5(c), (g), and (k) have been superposed on the plots to indicate the presence of two distinct class clusters). Figures 5(d), (h), and (l) represent the embedding images (a), (e), and (i) respectively in which intensity at every pixel in (a), (e), and (i) has been replaced by the 3 principal eigen values (e_1, e_2, and e_3) obtained via Graph embedding. Similar colored pixels in Figures 5(d), (h), and (l) correspond to the same class. The presence of two distinct colors (Figures 5(d), (h), and (l)) indicates clear separation between the lesion and shadowing classes (also indicated by labels L and S on 5(d), (h), and (l)). Comparing Figures 5(a), (e), and (i) with Figures 5(d), (h), and (l)

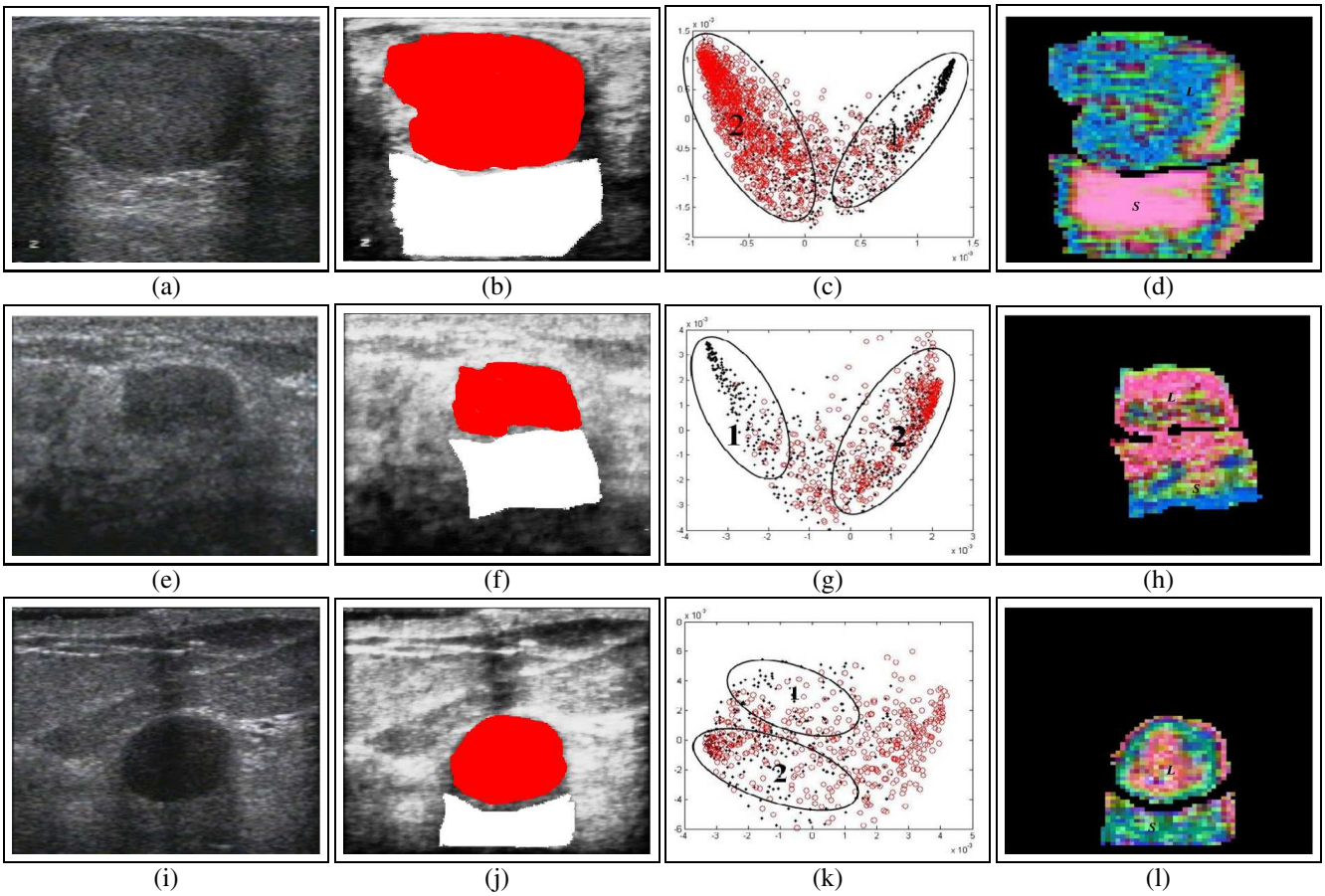

Fig. 5. (a), (e), (i) Original breast US images, (b), (f), (j) corresponding masks for lesion and PAS determined manually by a radiologist, (c), (g), (k) plot of the 2 principal eigen values (e_2 versus e_3) for the lesion (red dots) and PAS (black dots) classes, and (d), (h), (l) embedding images of (a), (e), (i) respectively in which intensity at every pixel in (a), (e), (i) has been replaced by the 3 principal eigen values obtained via Graph embedding.

suggests that the experts may have over segmented the lesion and PAS areas on the original breast US images, once again confirming that intensity information alone is not sufficient to discriminate between the two classes.

IV. Concluding Remarks

In this paper we have demonstrated that integrating several texture features at multiple scales and orientations can help accurately discriminate between lesions and shadowing. We also showed the utility of a non-linear dimensionality reduction method to visualize the separation between the lesion and shadowing clusters. We also quantitatively demonstrated via ROC analysis that the Boosted feature had superior discriminability between lesion and PAS compared to any single texture feature. Even though manually segmented masks with errors in labeling were used for the purposes of evaluation, we believe our conclusions are still valid. This work has significant clinical implications since the ability to distinguish between lesions and PAS will enable more accurate determination of lesion boundaries and hence improve classification of the lesion as benign or malignant by CAD algorithms or radiologists. In our approach we did not make a distinction between malignant and benign lesions even though it is known that different types of lesions differ in terms of echogenicity, texture, and intensity [1]. Future work will focus on applying our method to investigate differences between (a) benign and malignant lesions, (b) benign lesions and PAS, and (c) malignant lesions and PAS.

Acknowledgments

This work was supported by grants from the Wallace H. Coulter foundation (WHCF 4-29368, 4-29349) and the Offi ce of Technology Transfer (NJCST 4-21754) at Rutgers University.

References

[1] Stavros AT, Thickman et al. “Solid breast nodules: use of sonography to distinguish between benign and malignant lesions”, *Radiology*, vol. 196[1], pp. 123-34, 1995.

[2] A. Madabhushi, D. Metaxas, “Combining Low, High-Level and Empirical Domain Specifi c Knowledge for Automated Segmentation of Ultrasonic Breast Lesions”, *IEEE Trans. on Med. Imag.*, vol. 22[2], pp. 155-69, 2003.

[3] A. Madabhushi, D. Metaxas, “Ultrasound Techniques in Digital Mammography & Their Application in Breast Cancer Diagnosis”, *World Scientific Publn. Co.*, pp. 119-50, 2005.

[4] A. Madabhushi, J. Shi, *et al.* “Graph Embedding to Improve Supervised Classifi cation and Novel Class Detection: Detecting Prostate Cancer”, *MICCAI*, pp. 729-37, 2005.

[5] Drukker K, Giger ML, Mendelson EB, “Computerized analysis of shadowing on breast ultrasound for improved lesion detection”, *Med. Phys.*, vol. 30[7], pp. 1833-42, 2005.

[6] R. Duda, P. Hart, *Pattern Class. & Scene Anal.*, NY Wiley, 1973.

[7] Y. Freund, R. Schapire, “Experiments with a new Boosting Algorithm”, *Natl. Conf. on Machine Learning*, 1996, pp. 148-156.